RSC Advances

Role of acidic sites on beta-hexachlorocyclohexane (β-HCH) adsorption by activated carbons: molecular modelling and adsorption-desorption studies

SCHOLARONE™
Manuscripts

Role of acidic sites on beta-hexachlorocyclohexane (β-HCH) adsorption by activated carbons: molecular modelling and adsorption-desorption studies

A. Durimel[a], N. Passé-Coutrin[a], C. Jean-Marius[a], R. Gadiou[b], C. Enriquez-Victorero[c], D. Hernández-Valdés[c], U. Jauregui-Haza[c], S. Gaspard[a*]

[a]Laboratoire COVACHIM M2E, EA 3592 Université des Antilles et de la Guyane, BP 250, 97157 Pointe à Pitre, Cedex. Guadeloupe, French West-Indies, France.

[b] Institut de Science des Matériaux de Mulhouse, UMR CNRS 7361, 15 rue Jean Starky B.P.2488, 68057 Mulhouse Cedex, France

[c]Instituto Superior de Tecnologías y Ciencias Aplicadas, Salvador Allende y Luaces, La Habana, Cuba

*Corresponding author e-mail: sarra.gaspard@univ-ag.fr, Fax: +(590)590 48 3152,

Keywords: Hexachlorocyclohexane, activated carbon, adsorption isotherm, surface functional groups, molecular modelling, temperature programmed desorption.

Abstract:

The removal of β-HCH from contaminated water by adsorption on activated carbons is presented. Sugar cane bagasse activated carbons with different textural and surface chemical properties were prepared and characterized for studying β-HCH adsorption process. The isotherms are correlated by six models, among which the Fowler-Guggenheim/Jovanovic-Freundlich model is found to provide the best fit for two of the studied activated carbons. The isotherm adsorption data were correlated with the surface functional groups composition. β-

HCH adsorption was favored by the presence of acidic groups at the AC surface of chemically activated carbons. A throughout theoretical exploration of the potential energy surface for the interaction of β-HCH with a graphene sheet alone or containing hydroxyl or carboxyl surface groups were done. Molecular modelling results showed that under neutral to slightly acidic conditions only carboxylic surface groups should significantly contribute to β-HCH adsorption, in qualitative agreement with the experimental results. The analysis of the most stable structures suggests that the hydrogen bonds between the axial hydrogens of β-HCH and the charged oxygens of the deprotonated acidic surface groups are the main interactions responsible for the adsorption. This result is confirmed by a Temperature-Programmed Desorption study, showing that β-HCH molecules are associated with carboxylic groups of AC surface.

1. Introduction

Since 1960's, the French West Indian islands, Guadeloupe and Martinique have based their economy on two major agricultural productions: banana and sugar cane crops[1]. Indeed, tropical climate is favorable to production of banana, but it allows the development of parasite such as banana weevil (*Cosmopolite sordidus*) which attacks the roots of this plant. Indeed, to control this pest, chlorinated pesticides such as chlordecone (CLD), hexachlorocyclohexane (HCH) and dieldrine were used until the beginning of the 1990's, resulting in diffuse contamination of soils and surface waters[2]. HCH belongs to the organochlorinated compounds family. It is a monocyclic saturated chlorinated hydrocarbon of chemical formula $C_6H_6Cl_6$. The six chlorine atoms make it stable in the environment[3]. HCH is synthesised, by photochemical chlorination of benzene. The synthesis product, a mixture of HCH isomers (67-70% of α-HCH (alpha-HCH), 10 to 12% of γ-HCH or lindane, 5-6% of β-HCH (beta-HCH), 6% of δ-HCH, traces of ε-, λ-and υ-HCH) is called "technical" HCH. Lindane is the sole isomer having insecticide properties, nearly 90% of the HCH mixture are inactive

isomers[4], but all of them are toxic and carcinogenic[5]. Because of their low vapour pressure $(3,52.10^{-5}$ to $9,4.10^{-6}$ mm Hg), hexachlorocyclohexane isomers evaporate slowly from soil and surface waters. Their high sorption coefficient to organic carbon ($K_{oc} \approx 3.57$) gives them an excellent affinity for organic matter rich soils. When technical HCH is used, β-HCH isomer is the most persistent one due to the presence of chlorine atoms in equatorial position. β-HCH is highly accumulating and less easily degraded by living organisms[6-9]. Technical HCH was used since 1951 and its use was banned in France in 1972. Therefore, more than twenty years after HCH has been banned the molecule can be found in soils, water and the food chain in Guadeloupe and Martinica[2]. To limit impregnation to pesticides, in the polluted areas of Guadeloupe and Martinica, drinking water production plants were equipped with activated carbon filters.

Generally, adsorption on activated carbon is proved to be one of the most effective techniques in the separation and removal of a wide variety of organic micropollutants such as pesticides[10-11] from raw water. Despite its frequent use, AC remains an expensive material. Petroleum residues, natural coal and woods were for a long time, the main AC precursors[12-13]. But, since a few years, many lignocellulosic precursors at low cost and easily available have been used[14-23]. Sugar cane bagasse a by-product of sugar industry, has already been the subject of other studies[24-28]. Experiments using sugar cane bagasse allowed the production of ACs with good textural and adsorption properties[29]. The use of this renewable resource provides a sustainable cleaning process, because a high value product is obtained from a low cost material, and, simultaneously, it brings, solutions to the problem of wastes and local water pollution. Although some studies has been done on the removal of organo-chlorinated aromatics and pesticides by AC from contaminated water[10-11, 30-33]. There is very few information about the influence of surface functional groups on adsorption of this family of compounds by activated carbons. Adsorption of γ-HCH (lindane) has been studied on

different adsorbents such as bagasse ash[34], zeolithe[35], as well activated carbons[36-40]. In this research work, sugar cane bagasse activated carbons (SCB ACs) containing mainly large micropores, with different porous distribution and chemical groups composition at their surface were prepared and used to remove β-HCH from contaminated water. The influence of activated carbon surface properties and of textural characteristics on β-HCH adsorption onto SCB AC was explored. The adsorption data were correlated with the surface chemistry composition data obtained from X-ray photoelectron spectroscopy (XPS). The role of surface groups was also investigated by means of a theoretical approach and further comparison of experimental and theoretical results.

2. Materials and methods

2.1. Chemicals

β-hexachlorocychlohexane (98.5 %) was provided by Cluzeau Info Laboratory (C.I.L.). Critical size of β-HCH structurewas determined by using the MOPAC software.

2.2. Activated carbons: preparation

The ACs were obtained from sugar cane bagasse collected in Guadeloupe, French West Indies. These materials were initially dried at 105°C for 48 h using a drying oven, then ground and sieved to several particle sizes ranging from less than 0.2 to 1 mm. The fraction with a particle size ranging between 0.4 and 1 mm was used for carbonization. In this experiment, two conventional methods of preparation of AC were used. For physical activation, approximately 5 g of pre-treated sugar cane bagasse were initially pyrolyzed in a furnace Thermolyne F-21100 under nitrogen atmosphere at 800°C for 1 hour with a heating rate of 10°C/min. Carbon thus prepared, were then activated with steam under a nitrogen atmosphere at 800°C for 8 h with a heating rate of 10°C/min in the same furnace giving sample $BagH_2O$. For chemical activation, 3 g of the raw material was impregnated in phosphoric acid (H_3PO_4) 85% for 24 h, in order to facilitate the access of the acid

inside the particles. Impregnation ratios; X_P (g H_3PO_4 /g precursor): 0.5:1; 1:1 and 1.5:1 were used giving samples: BagP0.5, BagP1, BagP1.5 respectively. After impregnation, the samples were dried for 4 h at 110°C in a drying oven. The samples thus dried were pyrolyzed under a nitrogen flow at 600°C for 1 h. After cooling, until ambient temperature, the ACs thus obtained were washed with distilled water until stabilization of the pH.[41].

2.3. *Activated carbon: characterization*

The textural characterization of the produced ACs was carried out by N_2 adsorption at 77 K using a Micromeritics model ASAP-2020 analyzer. The microporous surface (S_{mi}) and external surface (S_{ext}), the total pore volume (V_T) and micropore volume (V_{mi}) were evaluated by the t-plot method, and mesopore volume (V_{me}) was estimated by the Barett-Joyner-Halenda (BJH) method[42]. The mean pore diameter, D_p, was calculated from $D_p = 4V_T/S$[43], where V_T, is the total volume of pores, and S being the BET surface area. The % of surface functional groups, O and C content, on the ACs surface were estimated by XPS (X-Ray Photoelectron Spectroscopy). XPS measurements were conducted on an Axis-Ultra DLD model Kratos, equipped with a hemispherical electron analyzer and Al-Kα (1253.6 eV) X-ray exciting source. The analysis of the C_{1s} and O_{1s} line allowed the semi-quantification of functional groups at the surface of the sample. Therefore, graphitic, hydroxyl, carbonyl and carboxyl groups were identified from the C_{1s} line. Further details were obtained from the O_{1s} line, particularly on carbonyl and hydroxyl groups and also on adsorbed water.

The total surface acidity and basicity of the samples were determined by titration with NaOH and HCl using the Boehm titration method[44] adapted by Moreno-Castilla et *al.*[45]. 0.2 g of AC was mixed with 50 ml of 0.05 N NaOH or HCl solutions for 48 h with continuous stirring. 10 ml of each filtrate were then titrated against 0.05N HCl or NaOH, using phenolphthalein as indicator. Capacity for H^+ and capacity for OH^- were then measured. The pH at point of zero charge (pH_{PZC}) was measured according to the procedure described in 46.

2.4.   *HCH quantification*

Quantification of β-HCH was carried out using a liquid chromatographer equipped with a mass spectrophotometer (AGILENT LC/MS 1100 series system). Ionization of β-HCH was achieved by electrospray (API-ES) in negative ion mode. Final parameters of nebulizer chamber were defined as following: drying gas flow: 12 L/min, temperature of drying gas: 350°C, pressure of atomizer: 35 psi, capillary tension: 4000 V, collision energy: 50 eV. The product-ion mass spectra of β-HCH are m/z 507 and 509. The LC/MS analyses were carried out using a C8 column (2,1 x 150 mm, Eclipse X08-C8). The LC separation was performed at 80°C using the following gradient: 0-6 min 55% of ACN in water, one minute more at 100%.

2.5.   *Adsorption isotherms*

To investigate the adsorption kinetic of β-HCH onto ACs surface, a stock solution at a concentration of 1 g.L^{-1} was prepared by dissolving β-HCH powder with pure acetone solution. For adsorption experiments, solutions were made by diluting from stock solution, to obtained aqueous solution at 1 mg.L^{-1}. Before adsorption experiments AC samples were first dried overnight at 105°C. Kinetic adsorption studies were performed in 500 mL of working volume of liquid sample contacting with 5 mg of each AC. Aqueous samples (1ml) were taken from the solution at preset time intervals and the concentrations were analyzed. For each experiment, two controls were prepared without bagasse AC, allowing studying the behavior of CLD, allowing to determine equilibrium time of adsorption (5 days). For adsorption equilibrium experiments, a fixed carbon mass (5 mg) was weighted into 200 mL conical flasks containing 100 mL of β-HCH solution at different initial concentrations ranging from 50 to 8000 μg.L^{-1}, agitated at 200 rpm and at 25±1°C until equilibrium was obtained. The equilibrium time was preliminary determined by kinetic tests. Each experiment was repeated at least two times under identical conditions. The amount of β-HCH adsorbed on the AC at equilibrium was calculated as:

$$q_e = V(C_0 - C_e)/M \qquad (1)$$

where q_e is the amount of adsorbate adsorbed at equilibrium per unit amount of adsorbent; V is the volume of aqueous β-HCH solution; C_0 is the initial concentration of β-HCH in liquid phase; C_e is the concentration of adsorbate in aqueous phase at equilibrium and M is the total mass of adsorbent.

2.6.   *Adsorption modeling*

The correlation of the experimental adsorption data with six adsorption models was undertaken to gain an understanding of the adsorption behaviour (Table 1). They can be classified into: (i) simple isotherm models for homogeneous surfaces without lateral interactions, like the Langmuir model[47]; (ii) isotherm models for homogeneous surfaces with lateral interactions, like the Fowler model[48]; (iii) isotherm equations for heterogeneous surfaces without lateral interactions, like Freundlich and Jovanovic-Freundlich models[49-50], (iv) isotherm equations for heterogeneous surfaces with lateral interactions, like the Fowler-Guggenheim/Jovanovic-Freundlich model[50], and (v) multilayer isotherm models for homogeneous surfaces without lateral interactions, like the multilayer Langmuir model[51].

Regressions of the experimental data to the adsorption isotherm models were performed using a corrected Newton algorithm[52]. The procedure calculates the values of the isotherm parameters which minimize the residual sum of squares (RSS):

$$RSS = \sum_{i=1}^{n} \left(q_{exp,i} - q_{t,i} \right)^2 \qquad (2)$$

where $q_{exp,i}$ and $q_{t,i}$ are the experimental and calculated values for each data point, respectively.

The selection of the most adequate model was performed using Fisher's test. The model selected exhibited the highest value of the Fisher parameter F_{calc}[52]:

$$F_{calc} = \frac{(n-l)\sum_{i=1}^{n}\left(q_{e,i}^{exp} - \overline{q_e^{exp}}\right)^2}{(n-1)\sum_{i=1}^{n}\left(q_{e,i}^{exp} - q_{e,i}^{t}\right)^2} \tag{3}$$

where $\overline{q_e^{exp}}$ is the mean value of the vector q_e^{exp} and l is the number of adjusted parameters of the model.

The average standard error of estimation (ASEE) is calculated as:

$$ASEE = \frac{100}{n} \cdot \sum_{i=1}^{n} \frac{|q_{exp,i} - q_{t,i}|}{q_{exp,i}} \tag{4}$$

2.7. *Temperature-programmed desorption (TPD) experiments*

ACs were first dried overnight at 105°C. A stock solution of β-HCH was prepared at 1 g/L dissolving β-HCH powder in pure acetone. Impregnation of pollutant was carried out adding 30 mg of AC in a β-HCH solution at concentration of 7 mg/L, to ensure a maximal adsorption. Once equilibrium was reached, the contaminated ACs were filtered and then dried at room temperature in a desiccator for 48h. Temperature programmed desorption (TPD-MS) was carried out in a vacuum device equipped with a line-of-slight detection quadrupole mass spectrometer[53-54]. TPD-MS tests were conducted with about 10 mg of each AC, before and after contamination by β-HCH. The acquisition of mass was done in a mass range of 1-200 units. To allow a precise quantification of desorbed gas, calibration of material was first made using four standard gases: H_2 (m/z = 2), CO (m/z = 28), CO_2 (m/z = 44) and H_2O (m/z = 18). The total pressure of the gas release during the heat treatment was measured as a function of the temperature. It was compared to the sum of the partial pressures of analyzed gases to allow a precise mass balance.

2.8. *Molecular modeling of β-HCH interactions with surface functional groups of AC*

In order to gain further understanding of the underlying interactions driving the adsorption process of β-HCH onto AC, several theoretical calculations with the modified Multiple Minima Hypersurface (MMH) methodology[55-56] were applied. This methodology allows exploring the interactions space of β-HCH with the functional surface groups of the AC (graphene, hydroxyl and carboxyl). This method combines quantum mechanical methods for the calculations of energy with statistical thermodynamics to obtain thermodynamic quantities related to the molecular association process. The AC is simulated by a simplified model: coronene without any surface group (graphene) and with different surface functional groups (hydroxyl and carboxyl). This model for AC does not take into account morphological or

topological characteristics of the AC, but it focuses on surface group interaction with adsorbate. The chemical changes produced in the functional groups at different pH were also taken into account. Since adsorption of HCH occurs from aqueous solution, the association energies for GRAPHENE/$(H_2O)_{n=0-3}$, OH/$(H_2O)_{n=0-3}$, COOH/$(H_2O)_{n=0-3}$, O$^-$/$(H_2O)_{n=0-3}$ and COO$^-$/$(H_2O)_{n=0-3}$ systems were calculated to be used as a reference. To study the adsorption of β-HCH onto AC and the influence of hydration conditions, the association energies for β-HCH/GRAPHENE/$(H_2O)_{n=0-3}$, β-HCH/OH/$(H_2O)_{n=0-3}$, β-HCH/COOH/$(H_2O)_{n=0-3}$, β-HCH/O$^-$/$(H_2O)_{n=0-3}$ and β-HCH/COO$^-$/$(H_2O)_{n=0-3}$ systems were calculated. The procedure explained in detail and all programs for processing are available on a web site[55, 57]. By comparison of the interaction energies for the surface group with water molecules or with water molecules and β-HCH it can be identified whether there is adsorption affinity between β-HCH and a given surface group.

The individual molecular structures where optimized by semi-empirical Hamiltonian PM6-DH2X as implemented in MOPAC2012[58]. Then, using the program GRANADAR2, 700 non redundant random configurations where generated for adsorbent–adsorbate clusters (the functional surface group of AC is modeled as adsorbent and the adsorbate molecules are β-HCH and/or water). Each of the initial random configurations generated was fully optimized with PM6-DH2X semi-empirical Hamiltonian using MOPAC2012. The results of the optimization process where statistically processed for calculation of the partition function and the thermodynamic quantities of molecular association i.e. thermodynamic association energy (E_{assoc}). Finally, by analyzing the populations of states of the optimized configurations, those structures that have a greater contribution to the macroscopic state of the studied system could be selected in order to identify the main interactions present.

3. Results

3.1. Characteristics of activated carbons

Parameters (specific surface area and pore volume) obtained for this SCB ACs have been extensively described in a previous paper[41]. The textural parameters presented have shown that SCB ACs were essentially mesoporous.

Surface functional groups of ACs are very important because they determine the surface properties of the carbons and, hence, their ability as ion exchangers, adsorbents, catalysts and catalyst supports[59]. The contents of carbon and oxygen, total amount of acidic groups as well as, total amount of basic groups at the bagasse activated carbons surface are presented in Table 2. XPS analysis was used for evaluation of chemical bonding states and concentrations of the surface functional groups formed on ACs surface (Table 3). Moreover, Table 2 shows that total basic groups and pH_{PZC} value decrease with increasing Xp values. The low values of pH_{PZC} are consistent with highest contents of acidic groups. The C_{1s} spectrum has been deconvoluted into five components with chemical shifts corresponding to: graphite type (284.1 – 184.4 eV), hydroxyl groups, or ether aromatic carbon (284.8 – 285.2 eV), carbonyl groups (285.5 – 286.1 eV), carboxyl and ester groups (286.3 – 287.6 eV) and a peak corresponding to π-π* transitions in the aromatic carbon (289.5 – 290.0 eV)[59-60]. The O_{1s} spectrum was fitted to three components: C=O groups (530 – 531.6 eV), C-OH or C-O-C groups (532.7 – 533.3 eV) and the last peak corresponding to chemisorbed oxygen (534.8 – 535.7 eV)[60-61]. The content of graphitic carbon increased with increasing Xp value.

3.2. Adsorption isotherms

The experimental adsorption data of β-HCH on the studied activated carbons at 298 K are plotted in Figure 1. The average relative error of the measured concentrations in the liquid phase was less than 5 % in all cases. The adsorption isotherm curves obtained for adsorption

of β-HCH on BagP0.5 and BagP1 are concave and reach a strict plateau. These curves correspond to a H-type isotherm[62] which is a limit form of the L-type isotherm (Figure 1). On the other hand, a sigmoidal curve with a point of inflection classified as a S-type isotherm was obtained for adsorption of β-HCH on BagP1.5 (Figure 1)[63].

Table 4 summarizes the results of the nonlinear regression analysis of the models evaluated in this work. In general, the agreement of the models with the experimental data is good as F_{calc} values show. The F_{calc} values obtained were larger for the regression of the Fowler-Guggenheim/Jovanovic-Freundlich and Fowler isotherm models than for the others studied. For Fowler-Guggenheim/Jovanovic-Freundlich model the average standard error of estimation was in the range of 4.4-7.8 %. Figure 1 shows the comparison between experimental adsorption data and values calculated using Fowler-Guggenheim/Jovanovic-Freundlich equation.

The high absolute values of χ, in both Fowler and Fowler-Guggenheim/Jovanovic-Freundlich equations, shows the importance of adsorbate-adsorbate interactions in the sorption process. Regarding the surface heterogeneity, it can be observed that the parameter ν in Freundlich, Jovanovic-Freundlich and Fowler-Guggenheim/Jovanovic-Freundlich models is different to unity for all supports. When the heterogeneity parameter is equal to unity, adsorption takes place on homogeneous surface. Then, as it can be expected, the ACs studied here have strongly heterogeneous surfaces. This fact is well known, due to both their pore size distribution and the presence of different functional groups on their surface[64-65]. It is thus not surprising that idealized models like Langmuir do not fit well the data for all investigated ACs, although Langmuir equation is still often used to analyze adsorption isotherms on such material. Moreover, the presence of several functional groups in the adsorbate molecule has been reported to diversify the interactions with activated carbon sites and thus to increase energy dispersion[65].

Even if the Fowler-Guggenheim/Jovanovic-Freundlich model describes pretty well the adsorption of β-HCH on BagP1.5, for describing this isotherm data the multilayer Langmuir model (MLM) was also used. This equation, based on the insertion of a constant *a* which represents the concentration on the x axis necessary to shift a Langmuir shaped isotherm that match part of the S type isotherm (Table 4), enables the estimation of q_s for each site.

The MLM gives a good agreement to the experimental data obtained with an F_{cal} value of 146.7 and an average error of estimation of 4.1% for the adsorption isotherm of β-HCH on BagP1.5 (Table 4). The S isotherm shape may be due to strong competition of the solvent molecules for the acidic surface sites and to moderate intermolecular interaction between the β-HCH molecules, but this last result also suggests that β-HCH adsorption on the BagP1.5 sample involves two adsorption sites. β-HCH molecules might have a lower affinity for the AC surface at low concentration and as the concentration of β-HCH increases, adsorption becomes easier.

3.3. Influence of textural and chemical properties of the ACs on β-HCH adsorption

The isotherms show that adsorption capacity increases with increasing acidic surface groups of the AC (Figure 4) and with increasing surface area (Table 4). It has been reported that the surface chemistry of the AC has to be considered an important factor in the adsorption mechanism of organics from diluted aqueous solutions[67-68].

Several works have been conducted in order to elucidate the adsorption mechanism of many molecules on different ACs. Those publications reveal that adsorption of organic molecules from dilute aqueous solutions on carbon materials is a complex interplay between electrostatic and non-electrostatic interactions and that both interactions depend on the characteristics of the adsorbent and adsorbate, as well as the solution chemical properties[67]. In the present work,

a theoretical approach used in order to elucidate the nature of β-HCH interaction with surface groups is discussed below.

The ACs prepared here contained significant amounts of both large micropores and mesopores and a mean pore diameter between 1.9 and 4.2 nm[41]. The pores are probably easily accessible to the sorbate molecule, according to the distance between the two farthest chlorine atoms, 6.23 Å, for the β-HCH molecule as depicted in Figure 2, and the mean pore diameter ≥ 1.9 nm. It is interesting to check the surface properties favoring the adsorption of a given molecule. Figure 2a shows clearly a linear increase of adsorption capacity of β-HCH on the ACs samples prepared by chemical activation with the amount of total acidic groups while the presence of hydroxyl groups may be detrimental to β-HCH adsorption (Figure 2b). No specific correlation with the amount of graphitic, carbonyl or ether groups was found. This correlation between the surface groups content and the adsorption capacity is in qualitative agreement with the theoretical prediction that at neutral or slightly acidic pH only carboxylic surface groups will favor the adsorption of β-HCH due to electrostatically driven interactions, as it will be discussed later.

On the other side, it is interesting to analyze the S form of BagP1.5 isotherm. The adsorption mechanism on BagP1.5 surface may involve first electrostatic interactions between the negatively charged oxygens of carboxylate surface groups and the axial protons of β-HCH followed to progressive association between the β-HCH molecules on the surface, giving a multilayer adsorption mechanism. This hypothesis is in agreement with the study of Lodge and Egyepong[69], showing that self-association of β-HCH molecules occurred in aqueous phase. This result is reinforced by the higher mean pore diameter of BagP1.5 (4.21 nm), the dimensions of β-HCH molecule (Figure 3) and the all-equatorial arrangement of chlorine atoms on the cyclohexane ring allowing packing of the β-HCH molecules.

3.4. TPD-MS study of interaction between β-HCH and ACs surface

TPD-MS profiles of raw and contaminated ACs were compared in order to understand interactions between the AC surface and β-HCH molecule. Total pressure, corresponding to the sum of all gases desorbed onto β-HCH contaminated ACs during the increasing of temperature, is compared to calculated pressure, which corresponds only to the sum of calibrated gases (H_2, H_2O, CO and CO_2). The difference between the measured and calibrated pressures $\Delta P = P_{mesaured} - P_{calculated}$ corresponds to desorption of a mixture of hydrocarbons, that is equivalent to the decomposition of adsorbed β-HCH. For all samples (Figure 4), maximum of desorption is observed at lower temperature (between 100 and 400°C) what could be related to the presence of molecules which are weakly interacting with ACs surface. Figure 5 enables to compare TPD-MS profile for raw and contaminated ACs both for CO and CO_2 desorption. For the three samples, CO curves show one peak at 200°C only for β-HCH contaminated ACs. Around 800°C, TPD profiles show a similarity between both samples but CO desorption is higher for raw ACs. Moreover, TPD curves for CO_2 desorption present the same profile for both samples but desorption is lower for the β-HCH contaminated AC, especially at 200-400°C and around 800°C. From these observations, one hypothesis could be proposed: β-HCH molecules are associated with carboxylic groups of AC surface which inhibit their desorption.

Furthermore, comparison of mass spectra of pure β-HCH, raw and contaminated ACs shows that mass spectrum of the pure β-HCH molecule is somewhat similar to those obtained when β-HCH is released from the AC surface. This would imply that β-HCH is physisorbed onto AC surface and no chemical bonds are formed between β-HCH and the surface. For all samples, desorption of HCl molecule can be observed. β-HCH is the only source of chlorine in contaminated material that can be attributed to its decomposition.

3.5 Molecular modeling of β-HCH interactions with surface functional groups of AC

Figure 6 summarizes the energy results obtained for β-HCH adsorption onto AC without water and with up to 3 water molecules. For neutral OH and COOH surface groups, the ΔE_{assoc} obtained in the presence of the contaminant is always higher or in the same order to that obtained for water molecules alone indicating lower or similar stability of the surface group/β-HCH complex compared to the surface group/water complex. Besides, for both neutral surface groups the system has similar stability with the β-HCH molecule alone or β-HCH plus up to three water molecules. This fact could be indicating a competition between water molecules and β-HCH molecules for the neutral surface groups. According to this, only a very small fraction of the contaminant will adsorb on a surface containing neutral OH and COOH SGs under real (very diluted) conditions, and thus, this surface groups will not contribute to increase the adsorption capacity. On the other hand, for the charged species of both surface groups, ΔE_{assoc} values are considerably lower in the presence of the contaminant, compared to the association of the AC model with water molecules alone (Figure 6a and b). Moreover, the stability of the systems surface group/β-HCH is considerably higher than surface group/β-HCH/$(H_2O)_{n=1-3}$ systems (although these are still energetically favored). This behavior suggests that if the β-HCH molecule is associated with the surface group, the water molecules will not be able to compete for the adsorption sites. The behavior is similar for both surface groups but the COO$^-$ affinity for the contaminant seems stronger. From this analysis, it can be suggested that the presence of charged surface groups will enhance the adsorption of β-HCH.

Additionally, Figure 6c shows the behavior of the ΔE_{assoc} for the graphene sheet. It can be seen that the clusters containing β-HCH are more stable than the GRAPHENE/$(H_2O)_{n=1-3}$ clusters. Despite the higher stability of the system when including the β-HCH molecule, the stability of these systems is not enough to drive the adsorption process.

The electrostatic interactions between the negatively charged surface groups and the area of positive electrostatic potential covering the three axial hydrogen[70] are most likely responsible for the adsorption process. An analysis of the distinctive minima structures, obtained for the systems $COO^-/\beta\text{-}HCH/(H_2O)_n$ and $O^-/\beta\text{-}HCH/(H_2O)_n$ (Figure 7), allows to conclude that almost all complexes show contacts between axial protons of β-HCH and negatively charged oxygen atoms of the surface groups. In addition to C-H$\cdots$O$^-$ interactions (Figure 7 COO$^-$/β-HCH-a, O$^-$/β-HCH-a), these complexes have water molecules interacting at the same time with negatively charged oxygen of SGs and axial protons of HCH molecules (Figure 7 COO$^-$/β-HCH/H$_2$O-a, O$^-$/β-HCH/H$_2$O-a). The water molecules interact with β-HCH through C-H$\cdots$OH$_2$ hydrogen bonds (Figure 7 COO$^-$/β-HCH/H$_2$O-a) or OH$\cdots$Cl bifurcated H-bonds (Figure 7 COO$^-$/β-HCH/(H$_2$O)$_2$-a), with the proton of water pointing to the region of negative electrostatic potential located between chlorine atoms. A similar bifurcated H-bond has been previously reported for the HF/HCH system[70].

For neutral complexes, all interactions described above for charged ones are also present, but structures with the β-HCH molecules directly situated above the surface group are much less common. Besides, interactions involving the π-cloud of the coronene derivative, such as C-H$\cdots\pi$ mainly with axial protons (Figure 9 COOH/β-HCH/H$_2$O-a, OH/β-HCH-a) and O-H$\cdots\pi$ (Figure 7 GRAPHENE/β-HCH/H$_2$O-a) are more commonly encountered compared with charged complexes.

According to association energies, the affinity order between HCH and the surface groups is as follows: COO$^-$>O$^-$>COOH$\approx$OH.

At pH $\approx$ 5-7, which is most likely the case for drinking water, a rough estimation gives a deprotonation of OH surface groups lower than 3%, that can be neglected, while only COOH groups are deprotonated to a considerable extent (~90 %)[71]. Taking into account that COO$^-$ is

the only charged surface group, it is predicted that carboxylic surface groups will be the main contributors to enhance β-HCH adsorption onto AC at neutral or slightly acidic pH conditions. This theoretical prediction is in agreement with the experimental results reported in this paper, namely, i) the evidences of TPD-MS study, ii) a linear increase of adsorption capacity of β-HCH with the amount of carboxylic groups while iii) the presence of hydroxyl groups may be detrimental to β-HCH adsorption and iv) the fact that nonspecific correlation with the amount of graphitic carbon was obtained. This agreement with the experimental results suggests that this theoretical approach can be used to preliminary screen different surface groups for the adsorption of a given contaminant.

4. Conclusion

The adsorption isotherms of β-HCH onto three different sugar cane bagasse activated carbons (BagP0.5, BagP1 and BagP1.5) obtained by activation with phosphoric acid impregnation, has been experimentally determined. The isotherms are correlated by six models, among which the Fowler-Guggenheim/Jovanovic-Freundlich model found to provide the best fit for two of studied activated carbons (BagP0.5, BagP1) with an average relative error of estimation between 4.2 % and 7.8 %. For the activated carbon BagP1.5, with a S type isotherm, the multilayer-Langmuir model was more adequate for describing the adsorption data of β-HCH with an average relative error of estimation of 4.1 %. Preliminary studies have been conducted in order to evaluate the differences in the surface chemistry of all activated carbons. For the samples prepared by chemical activation, a linear increase of adsorption capacity of β-HCH with the BET surface area and the amount of carboxylic groups was obtained, whereas, hydroxyl groups are detrimental to β-HCH adsorption, being these results in a fair qualitative agreement with the TPD-MS experimental evidences and with theoretical predictions from molecular simulations. Increasing the amount of acidic groups on the surface

by using high impregnation ratio, may increase β-HCH adsorption, nevertheless it may lead to an important increase of the mean pore diameter, that may reduce the surface area of the carbon and be detrimental for adsorption. No correlation with mesoporous, microporous volume, other oxygenated functionalities content or the graphitic carbon content was found. The analysis of the most representative structures obtained in the molecular modeling study allows the elucidation of the main interactions present between the surface groups and the β-HCH molecules, shedding some light upon the adsorption mechanism. These results reveal that the adsorption process of β-HCH on the highly acidic ACs might involve binding of the axial hydrogen atoms of β-HCH to deprotonated carboxylic groups through mainly electrostatic interactions. The adsorption mechanism on the most acidic sample, BagP1.5, might involve first H-bonding between the axial hydrogen atoms of β-HCH and the negatively charged acidic groups at the AC surface followed by progressive association between the β-HCH molecules. Future study to optimize β-HCH adsorption will focus on the modification of the carbon surface by creating carboxylic groups without, enlargement of the micropores.

Acknowledgments

References

1 J. Ganry, Comptes Rendus Biologies, 2004, **32**7, 621-627.

2 S. Coat, D. Monti, , P. Legendre, C. Bouchon, , F. Massat, G. Lepoint, Environ. Pollut., 2011, **159**, 1692-1701

3 M. Manickam, M. Mau, M. Schlömann, Appl. Microbiol. and Biotechnol., 2006, **69**, 580

4 K. Walker, D. Vallero, A.R. G. Lewis, 1999. Environ. Sci. Technol., 1999, **33** (24), 4373-4378.

5 A. K. Johri, M. Dua, D. Tuteja, R.Saxena, D. M. Saxena, R. Lal, Biotechnol. Letters, 1998, **20**, 885-887.

6 P. Sharma, V. Raina, R. Kumari, S. Malhotra, C. Dogra, H. Kumari, H. P.Kolher, H. R. Buser, C. Holliger, Appl. Environ. Microbiol., 2006, **72**, 5720-5727.

7 K. Kannan, Y. Yasunaga, H. Iwata, H. Ichihashi, S. Tanabe, R. Tatsukawa, Arch. Environ. Contam. Toxicol., 1995, **28**, 40-47.

8 T. M. Phillips, A. G. Seech, H. Lee, J. T. Trevors, Biodegradation, 2005, **16**, 363-392.

9 S.K. Sarkar, A. Binelli, C. Riva, M. Parolini, M. Chatterjee, A.K. Bhattacharya, B.D. Bhattacharya, K.K Satpath, Arch. Environ. Contam. Toxicol., 2008, **55**, 358-371.

10 O.A. Ioannidou, A.A. Zabaniotou, G.G. Stavropoulos, M.A. Islam, T.A. Albanis, Chemosphere, 2010, **80**, 1328-1336.

11 E. Ayranci, N. Hoda, Chemosphere, 2005, **60**, 1600-1607.

12 J. Guo, A.C. Lua, Materials Chemistry and. Physics, 2003, **80**, 114-119.

13 K. Amstaetter, E. Eek, G. Cornelissen, Chemosphere, 2012, **87**, 573-578.

14 J.H Tay, X.G. Chen , S. Jeyaseelan , N. Graham, Chemosphere, 2001, **44**, 45-51.

15 Y. Diao, W. P. Walawender, L. T. Fan, Bioresour. Technol., 2002, **81**, 45-52.

14 M. C. Baquero, L. Giraldo, J. C. Moreno, F. Suárez-García, A. Martínez-Alonso, J. M. D. Tascón, J. Anal. Appl. Pyrolysis, 2003, **70**, 779-784.

15 A.M. Youssef, N.R.E. Radwan, I. Abdel-Gawad, G.A.A. Singer, Colloids Surf., 2004, **252**, 143-151.

16 S. Babel, T.A. Kurniawan, Chemosphere, 2004**, 54**, 951-967.

17 K. Kadirvelu, C. Karthika, N.Vennilamani, S. Pattabhi,   Chemosphere, 2005, **60**, 1009-1017.

18 A. Namane, A. Mekarzia, K. Benrachedi, N. Belhaneche-Bensemra, A. Hellal¸ Journal of Hazardous Materials, 2005, **119**, 189-194.

19 S. Gaspard, S. Altenor, E.A Dawson., P. Barnes, A. Ouensanga, Journal of Hazardous Materials, 2007, **144**, 73-79.

20 S. Altenor, B. Carene-Melane, S. Gaspard, International Journal of Environmental Technology and Management, 2009, **10**, 308-326.

21 S. Altenor, B. Carene, E. Emmanuel, J. Lambert, J.J. Ehrhardt, S. Gaspard, Journal of Hazardous Materials, 2009, **165**, 1029-1039.

22 M.C. Ncibi, V. Jeanne-Rose, B. Mahjoub, J. Lambert, J.J. Ehrhardt, Y. Bercion, M. Seffen, S. Gaspard, Journal of Hazardous Materials, 2009, **165**, 240-249.

23 S. Nethaji, A. Sivasamy, Chemosphere, 2011, **82**, 1367-1372.

24 M. Valix, W.H. Cheung, G. McKay , Chemosphere, 2004, **56**, 493-501.

25 R.S. Juang, F.C. Wu, R.L. Tseng, Colloids Surf. A, 2002, **201**, 191-199.

26 W.T. Tsai , C.Y. Chang , M.C. Lin , S.F. Chien , H.F. Sun , M.F. Hsieh , Chemosphere, 2001, **45**, 51-58.

27 I.D. Mall , V.C. Srivastava , N.K. Agarwal , I.M. Mishra, Chemosphere, 2005, **61**, 492-501.

28 K. Zhang , W.H. Cheung , M. Valix, Chemosphere, 2005, **60**, 1129-1140.

29 I.D. Mall , V.C. Srivastava , N.K. Agarwal , Journal of Hazardous Materials, 2007, **143**, 386-395.

30 A. Bembnowska, R Pelech, E. Milchert, Journal of Colloid and Interface Science, 2003, **265**, 276-282.

31 K.Y. Foo, B.H. Hameed, Journal of Hazardous Materials, 2010, **175**, 1–11.

32 M.P. Ormad , N. Miguel , A. Claver , J.M. Matesanz , J.L. Ovelleiro , Chemosphere, 2008, **71**, 97-106.

33 Q. S. Liu , T. Zheng , P. Wang , J. P. Jian, N. Li , Chem. Eng. J., 2010, **157**, 348-356.

34 V. K. Gupta, C. K. Jain, I. Ali, S. Chandra, S. Agarwal, Water Res., 2002, **36**, 2483-2490.

35 Lemic J., Kovačević D., Tomašević-Čanović M.,.Kovačević Dr, Stanić T., Pfend R., 2006. Water Res., 2006, **40**, 1079.

36 J.L. Sotelo, G. Ovejero, J.A. Delgado, I. Martinez, Chem. Eng. J., 2002, **87**, 111-120.

37 J.L. Sotelo, G. Ovejero, J.A. Delgado, I. Martinez, Water Res., 2002, **36**, 599-608.

38 M. Akhtar, S.M. Hasany, M.I. Bhanger, S. Iqbal, Chemosphere, 2006, **66** (10), 1829-1838.

39 M. B. Ninkovic, R.D. Petrovic, M.D. Lausevic. Journal of Serbian Chemical Society, 2010, **75,** 565-573.

40 K. Ignatowicz. International Journal of Heat and Mass Transfer, 2011, **54**, 4931-4938.

41 N. Passé-Coutrin, S. Altenor, D. Cossement, C. Jean-Marius S. Gaspard, Microporous Mesoporous Materials, 2008, **111**, 1-3, 517-522

42 E.P. Barret, P.B. Joyner, P. Halenda, J. Am. Chem. Soc., 1951, **73**, 373-383,

43 M A. Díaz-Díez, V. Gòmez-Serrano, C. Fernández González, E. M. Cuerda-Correa, A., Macías Garcia, Appl. Surf. Sci., 2004, **238**, 309-313.

44 H.P. Boehm, E. Diehl, W. Heck, R. Sappock, Angewandte Chemie, 1964, **76**, 742-751.

45 C. Moreno-Castilla, F. Carrasco-Marin, E. Utera-Hidalgo, J. Rivera-Utrilla, Langmuir, 1993, **9**, 1378-1383.

46 M.V. Lopez-Ramon, F. Stoeckli, C. Moreno-Castilla, F. Carrasco-Marin, Carbon, 1999, **37**, 1215-1221.

47 I. Langmuir, J. Am. Chem. Soc., 1918, **40**, 1361-1403.

48 R. Fowler, E. A. Guggenheim, Statistical Thermodynamics, Cambridge University Press, Cambridge, 1965.

49 H. Freundlich, Zeitschrift fuer Physikalische Chemie, 1906, **57**, 384-470.

50 I. Quiñones, G. Guiochon, J. Coll. Interface Sci., 1996, **183**, 57-67.

51 P.G. Grant, S.L. Lemke, M.R. Dwyer, T.D. Phillips, Langmuir, 1998, **14**, 4292-4299.

52 S.L. Ajnazarova, V.V. Kafarov, Metodi Optimisatsi Eksperimenta v Khimicheskoy Teknologui, Vishaia Shkola, Moscow, 1985.

53 R. Gadiou, E.A. Dos Santos, M. Vijayaraj, K. Anselme, J. Dentzer, G.A. Soares, C. Vix-Guterl. Colloids Surf. B, 2009, **73**, 168-174.

54 P. Brender, R. Gadiou, J.-C. Rietsch, P. Fioux, J. Dentzer, A. Ponche, C. Vix-Guterl. Anal. Chem., 2012, **84**, 2147-2153.

55 L.A. Montero, A.M. Esteva, J. Molina, A. Zapardiel, L. Hernández, H. Márquez, A. Acosta, J. Am. Chem. Soc., 1998, **120**, 12023-12033.

56 D. Hernández Valdés, C. Enriquez Victorero, U. Jáuregui Haza, P. Hernández Valdés, S. González Santana. Revista Cubana de Ciencias Informáticas, 2013, **7**, 9-15.

57Available by request: <http://karin.qct.fq.oc.uh.cu/mmh/>

58 Stewart, J.J.P. MOPAC2012, Stewart Computational Chemistry. Stewart Computational Chemistry, Colorado Springs, CO, USA, 2012.

59 T. Budinova, E. Ekinci, F Yardim., A. Grimm, E. Björnbom, V. Minkova, M. Goranova, Fuel Process. Technol., 2006, **87**, 115-124.

60 S. Figaro, S. Louisy-Louis, J. Lambert, J.-J. Ehrhardt, A. Ouensanga, S. Gaspard, Water Res., 2006, **40**, 3456-3466.

61 W. Jung, K.H Ahn., Y.Lee, K.P. Kim, J.S. Rhee, J. T Park. . K.J Paeng, Microchem. J., 2001, **70**, 123-131.

62 C. H. Giles, T. H. MacEwan, S. N. Nakwa, D.J. Smith, J. Chem. Soc., (1960) 3973-3993. DOI: 10.1039/JR9600003973

63 G. Limousin, J.-P. Gaudet , L. Charlet , S. Szenknect , V. Barthès , M. Krimissa,   Appl. Geochem., 2007, **22**, 249-275.

64 M. Dabrowski, P. Podkościelny, Z. Hubicki, M. Barczak. Chemosphere, 2005, **58**, 1049-1070.

65 K. László, P. Podkościelny, A. Dabrowski. Appl. Surface Sci., 2006, **252**, 5752-5762.

66 A. Derylo-Marczewska, S. Swiatkowski, M. Biniak, Walczyk, Colloids Surf. A, 2008, **327**, 1-8.

67 C. Moreno-Castilla, Carbon, 2004, **42**, 83-94.

75 C. Quesada-Penatea, U. Julcour-Lebigue, A.M. Jáuregui-Haza, Wilhelm, H. Delmas, Chem. Eng. J., 2009, **152**, 183–188.

68 K.B. Lodge, E.J. Egyepong. J. Phys. Chem. A, 2010, **114**, 5132–5140.

69 C. Ouvrard, M. Luçon, J. Graton, M. Berthelot, C. Laurence, J. Phys. Organic Chem., 2004, **17**, 56-64.

70 D.R. Lide, CRC Handbook of Chemistry and Physics, Internet Version 2005, CRC press, 2005.

Figure captions

Figure 1: Adsorption isotherm of β-HCH onto three sugarcane activated carbons at 298 K.

Figure 2: Comparison between experimental adsorption isotherms of β-HCH (symbols) and calculated values (lines) for different sugar cane bagasse activated carbons at 25°C. For BagP0.5 and BagP1 the best fit was obtained for Fowler-Guggenheim/Jovanovic-Freundlich model. For BagP1.5 the multilayer Langmuir model was used. q_e is the amount of adsorbate adsorbed at equilibrium per unit amount of adsorbent (µg/mg) and C_e is the concentration of adsorbate in aqueous phase at equilibrium (µg/L).

Figure 3: Structure of β-HCH molecule. Calculated critical dimensions: x = 6.23 Å, y = 5.62 Å and y = 3.67 Å.

Figure 4 : β-HCH adsorption capacity plotted against percentage of surface groups : a) acidic groups   b) hydroxyl groups

Figure 5: Difference between the measured and calculated pressures $\Delta P = P_{calculated} - P_{meseaured}$ obtained during TPD–MS experiments for (▲) BagP0.5, (♦) BagP1 and (●) BagP1,5.

Figure 6: Temperature programmed desorption profiles for raw and β-HCH contaminated sugarcane activated carbons: BagP0,5, BagP1 and BagP1,5.

Figure 7: Thermodynamic association energy (ΔE_{assoc}) for the systems surface group/$(H_2O)_{n=0-3}$ and surface group/β-HCH/$(H_2O)_{n=0-3}$ including the charged forms of surface groups: a) carboxylic and carboxylate surface groups; b) hydroxyl and hydroxylate surface groups; c) graphene sheet.

Figure 8: Some representative minima structure illustrating the main interactions between β-

HCH, surface groups in either charged or neutral form and water molecules.

1

2

3

1

Figure 1. Comparison between experimental adsorption isotherms of β-HCH (symbols) and calculated values by Fowler-Guggenheim/Jovanovic-Freundlich equation (lines) for different sugarcane bagasse activated carbons at 25°C.
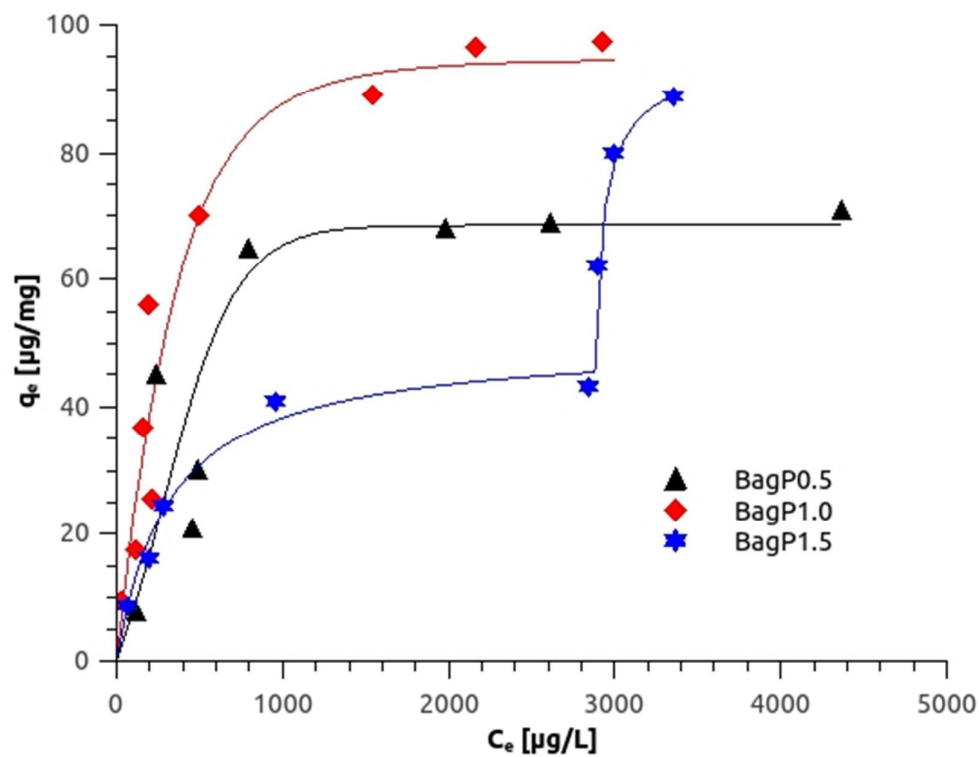
Figure 2: Influence of chemical properties of activated carbons onto β-HCH adsorption. Influence of (a) percentage of acidic groups and (b) hydroxyls groups onto adsorption capacity.
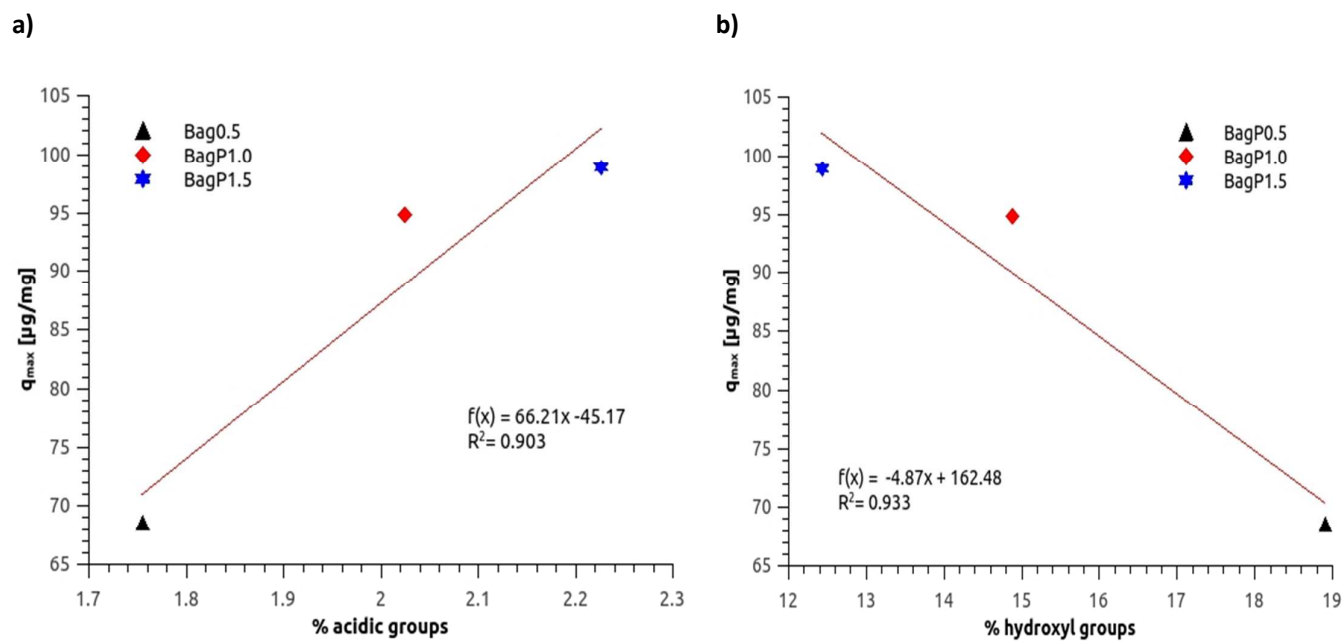
a)

$f(x) = 66.21x - 45.17$
$R^2 = 0.903$

b)

$f(x) = -4.87x + 162.48$
$R^2 = 0.933$

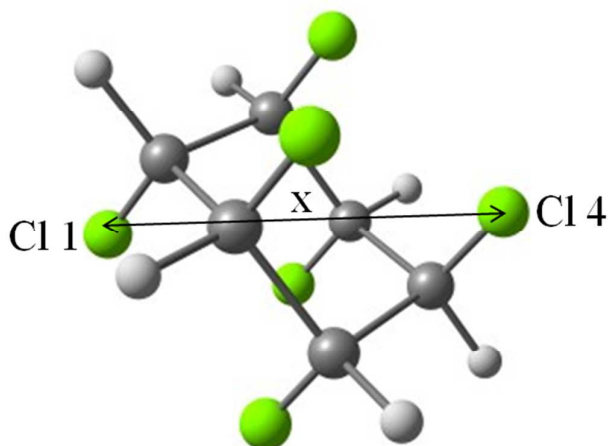Figure 3: Structure of β-HCH molecule. Calculated critical dimensions: x = 6.23 Å, y = 5.62 Å and z = 3.67 Å.

Figure 4. Difference between the measured and calculated pressures $\Delta P = P_{calculated} - P_{meseaured}$ obtained during TPD–MS experiments for (▲) BagP0.5, (♦) BagP1 and (●) BagP1,5.
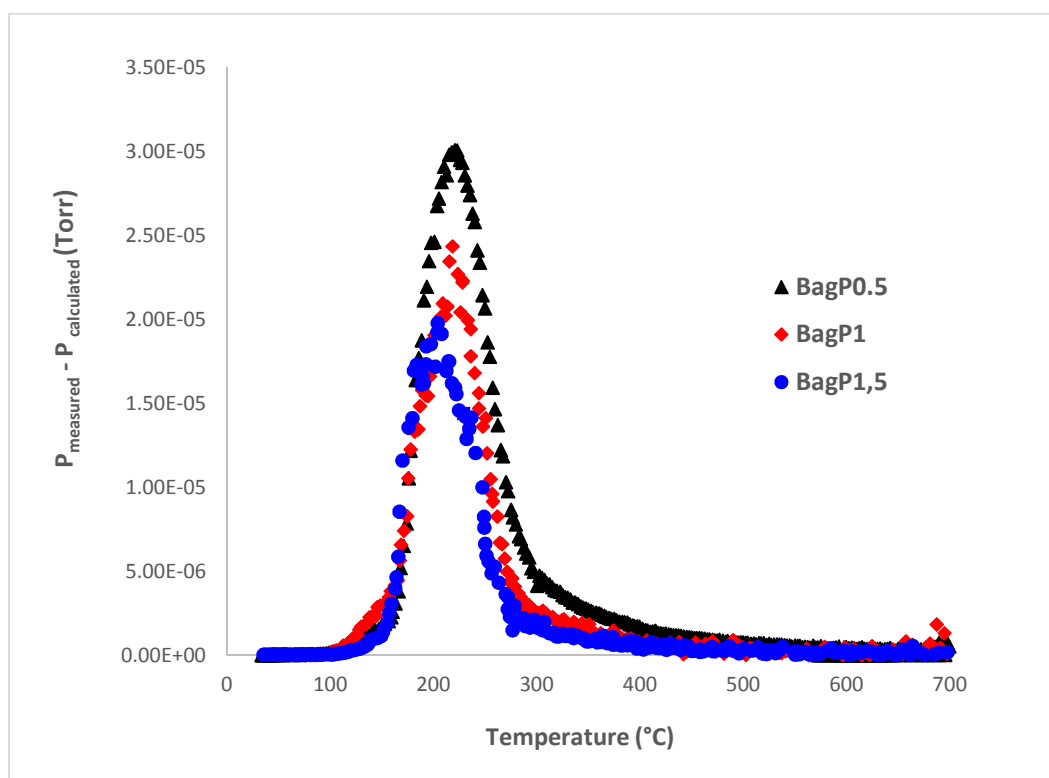
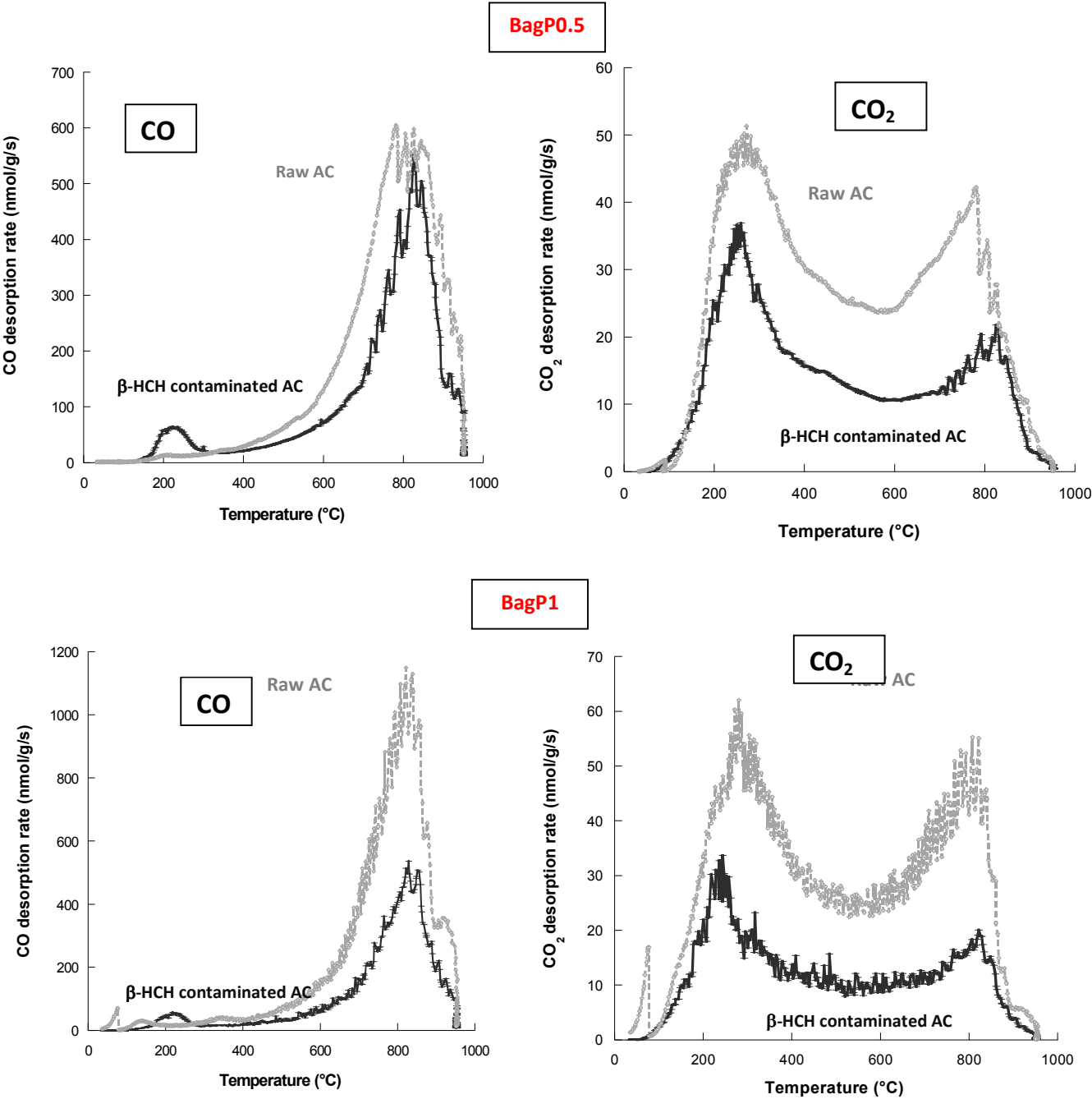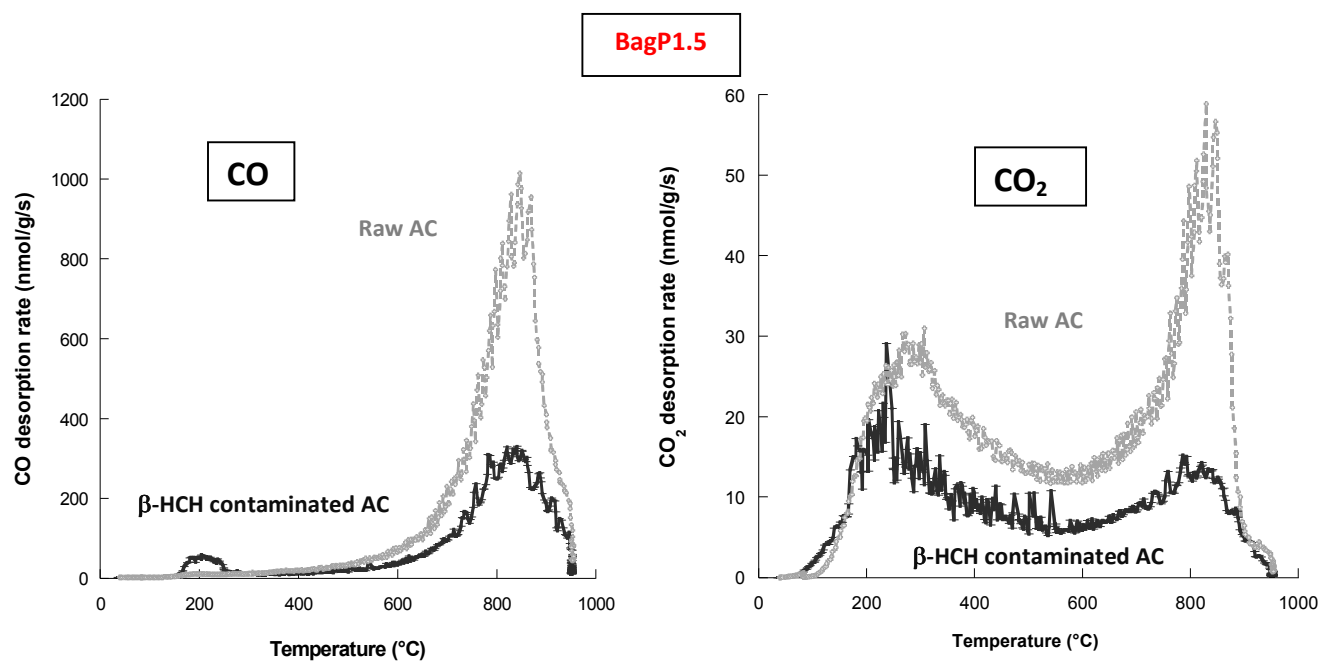Figure 5. Temperature programmed desorption profiles for raw and β-HCH contaminated sugarcane activated carbons.

Figure 6. Thermodynamic association energy (ΔE_{assoc}) for the systems surface group/$(H_2O)_{n=0-3}$ and surface group/β-HCH/$(H_2O)_{n=0-3}$ including the charged forms of surface groups: a) carboxylic and carboxylate surface groups; b) hydroxyl and hydroxylate surface groups; c) graphene sheet.
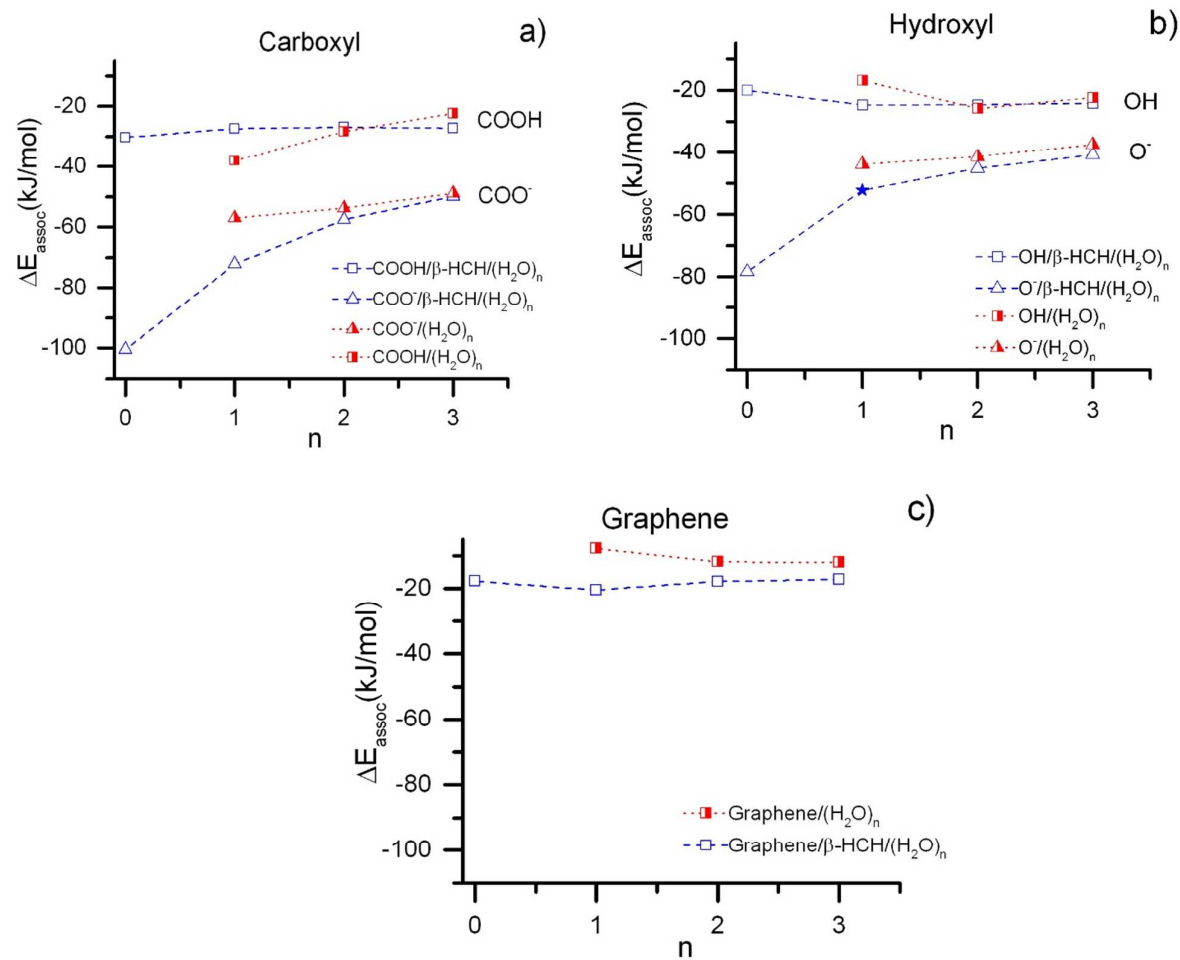
Figure 7. Some representative minima structure illustrating the main interactions between β-HCH, surface groups in either charged or neutral form and water molecules.

COO⁻/β-HCH-a   COO⁻/β-HCH/H₂O-a   COO⁻/β-HCH/H₂O-b   COO⁻/β-HCH/(H₂O)₂-a   COO⁻/β-HCH/(H₂O)₃-a

O⁻/β-HCH-a   O⁻/β-HCH/H₂O-a   O⁻/β-HCH/(H₂O)₂-a   COOH/β-HCH-a

COOH/β-HCH/H₂O-a   COOH/β-HCH/(H₂O)₃-a   OH/β-HCH-a   OH/β-HCH/H₂O-a

OH/β-HCH/(H₂O)₃-a   GRAPHENE/β-HCH-a   GRAPHENE/β-HCH/H₂O-a   GRAPHENE/β-HCH/H₂O-b
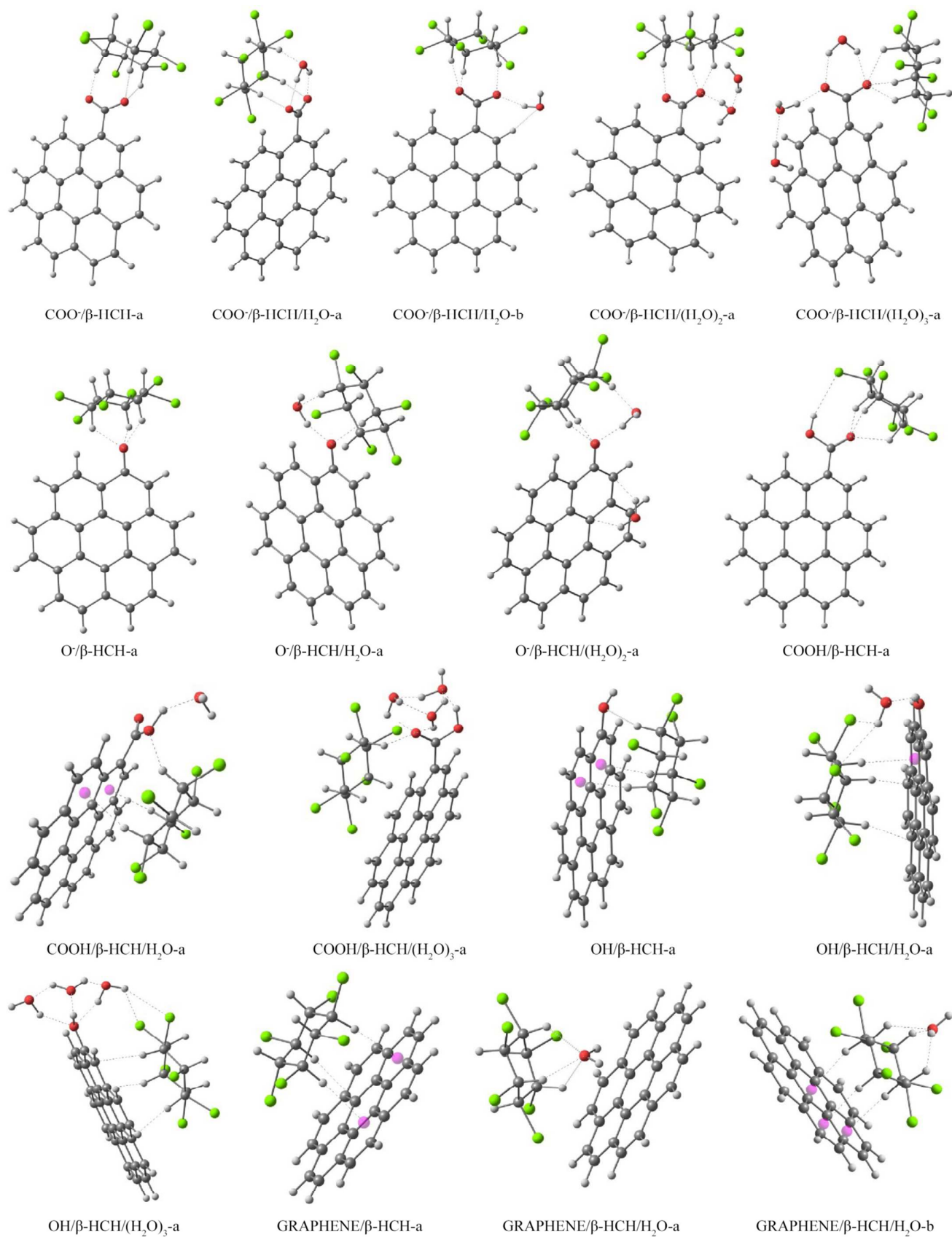
Table 1: Adsorption isotherm models

Model	Equation*
Langmuir	$q_e = q_s K c_e / (1 + K c_e)$
Fowler	$q_e = q_s K c_e / (e^{-\chi q_e / q_s} + K c_e)$
Freundlich	$q_e = K c_e^{v}$
Jovanovic-Freundlich	$q_e = q_s (1 - e^{-(K c_e)^{v}})$
Fowler-Guggenheim/Jovanovic-Freundlich	$q_e = q_s (1 - e^{-\left(K c_e e^{\chi q_e / q_s}\right)^{v}})$
Multilayer Langmuir	$q_e = (q_{s1} K_1 c_e / (1 + K_1 c_e)) + (q_{s2} K_2 (c_e - a) / (1 + K_2 (c_e - a)))$

*q_e is the amount of adsorbate adsorbed at equilibrium per unit amount of adsorbent, q_s is the monolayer capacity, C_e is the concentration of adsorbate in aqueous phase at equilibrium, χ is the adsorbate-adsorbate interaction parameter, v is the heterogeneity parameter, K and a are other parameters.

Table 2: Chemical characteristics of sugar cane bagasse activated carbons obtained by XPS, and Boëhm titration.

Sample	Composition (%)			Acidic groups (meq/g)	Basic goups (meq/g)	pH$_{PZC}$
	C	O	O/C			
BagP0.5	87.06	9.06	0.10	1.755	0.250	3.83
BagP1.1	87.71	9.05	0.10	2.025	0.187	3.79
BagP1.5	88.88	7.92	0.09	2.227	0.062	3.52

Table 3: Surface functional groups of sugar cane bagasse AC obtained by XPS

Sample	Graphitic *284.1 – 284.4 eV*	Hydroxyl *284.8 – 285.2 eV*	% Functional groups from C_{1s} spectra			% Functional groups from O_{1s} spectra deO_{1s}		
			Carbonyl *285.5 – 286.1 eV*	Carboxyl *286.3 – 287.6 eV*	π-π* *289.5 – 290.0 eV*	C=O 530 – 531.6 eV	C-OH or C-O-C 532.7 – 533.3 eV	chimiosorbed Oxygen 534.8 – 535.7 eV
BagP0.5	55.92	18.91	14.43	5.87	4.87	22.40	47.04	25.05
BagP1	56.32	14.89	14.52	7.67	6.61	21.23	51.67	23.52
BagP1.5	66.25	12.43	8.60	6.78	5.94	34.69	43.35	21.97

Table 4 : Isotherm model parameters (along with 95% confidence intervals) and goodness of fit.

Model and parameters*			
	BagP0.5	BagP1	BagP1.5
1.- Langmuir			
q_s, $\mu g/mg_{AC}$	83.2±4.7	108.2±8.3	93.9±6.4
K, $L/\mu g$	0.0019±0.0001	0.0031±0.0002	0.00091±0.00007
ASEE	31.6	18.2	20.1
F_{calc}	5.2	15.1	6.0
2.- Fowler			
q_s, $\mu g/mg_{AC}$	69.3±4.3	95.8±5.9	89.5±6.2
K, $L/\mu g$	0.00015±0.00002	0.0011±0.0003	0.00028±0.00004
χ	5.83±0.38	2.83±0.17	2.03±0.16
ASEE	11.0	12.5	30.3
F_{calc}	84.9	46.2	7.1
3.- Freundlich			
K, $\mu g^{1-\nu} L^{\nu} mg_{AC}^{-1}$	4.60±0.27	5.24±0.39	1.11±0.08
ν	0.34±0.04	0.38±0.04	0.52±0.09
ASEE	44.0	30.6	15.0
F_{calc}	4.1	9.5	6.9
4.- Jovanovic-Freundlich			
q_s, $\mu g/mg_{AC}$	71.6±5.1	95.7±6.3	93.6±4.6
K, $L/\mu g$	0.0016±0.0002	0.0025±0.0003	0.0005±0.00012
ν	0.93±0.07	1.01±0.08	0.71±0.05
ASEE	28.8	18.4	13.6
F_{calc}	4.6	14.1	5.5
5.- Fowler-Guggenheim/Jovanovic-Freundlich			
q_s, $\mu g/mg_{AC}$	68.5±5.4	94.8±5.9	98.9±6.1
K, $L/\mu g$	0.000025±0.000003	0.000061± 0.000013	0.000011± 0.000002

χ	7.73±0.38	6.20±0.43	5.80±0.47
ν	0.46±0.04	0.41±0.03	0.30±0.01
ASEE	4.2	7.5	7.8
F_{calc}	156.8	76.8	39.4
6.- MultilayerLangmuir			
q_{s1}, µg/mg$_{AC}$	-	-	50.3±2.1
K_1, L/µg	-	-	0.0032±0.0002
q_{s2}, µg/mg$_{AC}$	-	-	94.6±4.6
K_2, L/µg	-	-	0.030±0.0024
a, µg/L	-	-	2838±78
ASEE	-	-	4.1
F_{calc}	-	-	146.7

*qs is the monolayer capacity, χ is the adsorbate-adsorbate interaction parameter, ν is the heterogeneity parameter, K and a are other parameters, ASEE is the Average Standard Error of Estimation, Fcal is the calculated Fisher parameter.